Showcasing research from Dr. Sun's laboratory, Advanced Biofuels and Bioproducts Process Development Unit, Biological Systems and Engineering Division, Lawrence Berkeley National Laboratory, USA.

Volatile fatty acid extraction from fermentation broth using a hydrophobic ionic liquid and *in situ* enzymatic esterification

Volatile fatty acids (VFAs) produced using wastewater carbon from animal farms can be efficiently extracted and esterified using a hydrophobic ionic liquid.

As featured in:

See Ning Sun *et al.*, *RSC. Sustainability.*, 2025, **3**, 311.

ROYAL SOCIETY OF CHEMISTRY

rsc.li/rscsus

Registered charity number: 207890

RSC Sustainability

ROYAL SOCIETY OF CHEMISTRY

PAPER

View Article Online
View Journal | View Issue

Cite this: *RSC Sustainability*, 2025, **3**, 311

Volatile fatty acid extraction from fermentation broth using a hydrophobic ionic liquid and *in situ* enzymatic esterification

Ramkrishna Singh, [ab] Nikhil Kumar,[cd] Prathap Parameswaran,[e] Blake A. Simmons, [bd] Kenneth Sale[cd] and Ning Sun *[ab]

Received 5th July 2024
Accepted 9th September 2024

DOI: 10.1039/d4su00346b

rsc.li/rscsus

Efficient recovery of volatile fatty acids (VFAs) from fermentation broth is a challenge due to low VFA titers and thus limits the commercialization of VFA production using biological routes. Liquid–liquid extraction using hydrophobic ionic liquids (ILs) shows great promise for the extraction and esterification of hydrophilic VFAs. In this study, several ILs were evaluated to select a water-immiscible and efficient extraction solvent. The selected IL, trihexyltetradecyl phosphonium dibutylphosphate ([$P_{666,14}$][DBP]), gave a cumulative VFA extraction of around 842.8 mg per g IL. The predicted excess enthalpy (H^E) and logarithmic activity coefficients ln(γ) using the COSMO-RS model were validated with the experimentally obtained VFA recovery from fermentation broth. To understand the extraction mechanism of VFAs, quantum theory of atoms in molecules (QTAIM) and noncovalent interaction (NCI) were performed. The results suggest that long chain fatty acids exhibit strong van der Waals interaction with the DBP anion leading to higher VFA extraction. The enzymatic esterification of VFAs with ethanol in [$P_{666,14}$][DBP] was optimized using the Box–Behnken response surface design of experiment. Under the optimized conditions, up to 83.7% of hexanoic acid was converted to ethyl esters, while other shorter chain VFAs have lower conversion efficiency (38.3–63.2%).

Sustainability spotlight

Wastewater from animal farms and organic wastes can be fermented to produce volatile fatty acids (VFAs) for carbon utilization and resource recovery. This work developed a greener approach for VFA extraction from aqueous media by replacing organic solvents with hydrophobic ionic liquids. *In situ* esterification of VFAs using immobilized enzymes was also demonstrated to facilitate the final product recovery. This work supports the United Nations Sustainable Development Goals, particularly SDG 12 (Sustainable consumption and production patterns) and SDG 13 (Climate change), by reducing the carbon footprint and using greener production processes.

1 Introduction

Wastewater generated from large-scale animal farms provides an opportunity for the recovery of carbon and other nutrients.[1] The wastewater carbon can be upgraded to VFAs using mixed microbial cultures.[2,3] VFAs are widely used as raw materials in food, pharmaceutical, and chemical industries,[2,4] and serve as carbon sources or precursors for production of biofuels[5] and bioplastics.[6] They can also be converted to other derivatives including alcohols, esters, and aldehydes.[7] VFAs produced from petroleum sources contribute about 3.3 tons of CO_2 equivalent per ton.[8] Therefore, alternative feedstocks such as food waste, waste sludge, wastewater, and agricultural residues have been utilized to improve the sustainability of VFA production through bioconversion.[9]

Economical VFA separation and recovery after bioprocessing is challenging due to the low titers of VFAs. Different separation techniques such as resin adsorption, distillation, pervaporation, liquid–liquid extraction, and membrane-based separation have been applied to VFA separation from fermentation broth and waste streams.[8] Affinity separation techniques such as liquid–liquid extraction provide an opportunity for effective separation and recovery of the components from dilute streams. Hydrophobic ionic liquids (ILs) are greener alternatives for VFA recovery with higher extraction efficiencies compared to organic

[a]*Advanced Biofuels and Bioproducts Process Development Unit, Lawrence Berkeley National Laboratory, 5885 Hollis Street, Emeryville, CA 94608, USA. E-mail: nsun@lbl.gov*

[b]*Biological Systems and Engineering Division, Lawrence Berkeley National Laboratory, 1 Cyclotron Road, Berkeley, California 94720, USA*

[c]*Biosecurity and Bioassurance Department, Sandia National Laboratories, 7011 East Avenue, Livermore, CA 94551, USA*

[d]*Joint BioEnergy Institute, Lawrence Berkeley National Laboratory, 5885 Hollis Street, Emeryville, CA, 94608, USA*

[e]*Department of Civil Engineering, Kansas State University, 2118 Fiedler Hall, 1701C Platt Street, Manhattan, KS 66506, USA*

solvents such as alcohols, ketones, aliphatic hydrocarbons, and aliphatic amines.[10–13] Certain ILs have been reported for the extraction of VFAs from both model solution and actual fermentation broth.[13–16] Esters of VFAs have lower water solubility and boiling points compared to hydrophilic VFAs, allowing distillation with lower energy input.[15] In 2019, the US ester market was valued at USD 3.8 billion, and is estimated to reach USD 5 billion by 2025.[17] Short-chain esters are used in food, brewery, and pharmaceutical products for their flavor and fruity fragrance. Conventionally, the acid-catalyzed process is used for ester manufacturing. However, this process causes equipment corrosion and raises environmental concerns due to wastewater generation.[18] Therefore, alternative approaches including enzymatic esterification of VFAs with alcohols, and microbial ester production have been investigated.[19] Since enzymatic esterification of VFAs in water is reversible, the reaction is only feasible in a hydrophobic solvent. Hydrophobic ILs, such as those containing phosphonium or ammonium cations and phosphinate or carboxylate anions, are potential solvents for VFA extraction.[20] Additionally, hydrophobic ILs also act as reaction media for the esterification of VFAs. With different structures of the ILs and concentrations of ILs/VFAs several mechanisms including (a) competitive extraction of VFA and water, (b) non-competitive VFA extraction, and (c) co-extraction of water with VFAs have been proposed.[21] Extraction and acid-catalyzed esterification of acetic acid in ILs have been reported using different anions with the trihexyl(tetradecyl) phosphonium ($[P_{666,14}]^+$) cation. The authors observed that dicyanamide (DCA) and chloride (Cl) anions gave higher extraction values but the esterification efficiency was negligible. On the other hand, higher esterification efficiency was achieved using tetrafluoroborate (BF_4) (75%) and bis(trifluoromethylsulfonyl)-imide (Tf_2N) (85%), although extraction efficiency was low. A mixture of $[P_{666,14}]Cl$ and $[P_{666,14}][Tf_2N]$ was suggested to achieve extraction efficiency similar to DCA and Cl while achieving about 56% esterification.[15] Using Brønsted acidic IL as a catalyst, 30–67% conversion of acetic acid into butyl acetate was achieved under different experimental conditions.[22]

This study aims to identify a suitable hydrophobic IL that can not only effectively extract VFAs but also facilitate the *in situ* esterification. Furthermore, the effect of the pH of the substrate on VFA extraction was assessed. Thermodynamic properties, including excess enthalpy and activity coefficient, were computed using the COnductor like Screening MOdel for Real Solvents (COSMO-RS) approach and served as a basis for evaluating solvent efficacy in VFA extraction from aqueous media. To elucidate the extraction mechanism, quantum chemical simulations were conducted to understand the interactions of ILs with VFAs. Quantum Theory of Atoms in Molecules (QTAIM), Reduced Density Gradient (RDG), and Noncovalent Interactions (NCI) analysis were implemented to dissect the role of weak interactions and characteristics of IL–VFA interactions associated with efficient VFA extraction. The enzymatic esterification of VFAs using immobilized *Candida antarctica* lipase B and ethanol in the selected IL was optimized using a response surface methodology. Thus, this study demonstrated an integrated extraction and esterification of VFAs from a dilute aqueous fermentation broth using a functionalized hydrophobic IL.

2 Materials and methods

2.1. Materials

Chemicals including acetic acid (≥99.7%), propionic acid (≥99.5%), butyric acid (≥99%), hexanoic acid (≥99%), and anhydrous ethanol (200 proof, ≥99.5%) were procured from Millipore Sigma (WI, USA). ILs including trihexyltetradecyl phosphonium dibutylphosphate ($[P_{666,14}][DBP]$, 95%), trihexyltetradecyl phosphonium chloride ($[P_{666,14}]Cl$, 95%), trihexyltetradecyl phosphonium dimethylphosphate ($[P_{666,14}][DMP]$, 95%), tributylhexyl phosphonium chloride ($[P_{444,6}]Cl$, 95%), tributylmethyl phosphonium bis-2,4,4-trimethylpentyl phosphonium ($[P_{444,1}][TMP]$, 97%) and 1-dodecyl-3-methylimidazolium dicyanamide ($[C_{12}C_1IM][DCA]$, 97%) were purchased from IOLITEC GmbH (Heilbronn, Germany). Novozym 435 (immobilized *Candida antarctica* lipase B) with enzyme activity of 11 100 propyl laurate unit (PLU) per g was provided by Novozymes North America Inc., (NC, USA).

2.2. Ionic liquid selection

A known amount of ILs among $[P_{666,14}][DBP]$, $[P_{666,14}]Cl$, $[P_{666,14}][DMP]$, $[P_{444,6}]Cl$, $[P_{444,1}][TMP]$ and $[C_{12}C_1IM][DCA]$ was brought into contact with distilled water at 1 : 1 ratio and vortexed for 5 min at 1500 rpm. The IL–water mixture was observed for phase separation after being allowed to stand for 5 min. A suitable IL was selected for this study based on its immiscibility in water.

2.3. VFA extraction using selected ILs

To determine the extraction efficiency of VFAs in the selected ILs, an aqueous VFA model solution was prepared containing 0.8% w/v of acetic acid, propionic acid, butyric acid, and hexanoic acid each (limited by the solubility of hexanoic acid in water). The model solution (1 ml) was combined with 100 mg of the selected IL and mixed at 2000 rpm for 1 h. At the end of 1 h, the mixture was centrifuged at 4000 rpm for 5 min to obtain two separate phases. An aliquot of the aqueous phase was carefully pipetted and used for residual VFA quantification. The difference in VFA concentration in the aqueous phase was used to calculate the extraction of VFAs in each IL. The IL phase (containing extracted VFA) was separated and combined with a fresh model solution to determine the maximum extraction capacity of VFAs in the IL. The maximum VFA extraction in the IL was also investigated at different initial pH values of the model solution. A 0.8% w/v model solution was prepared and the initial pH was adjusted to 1.5, 3.0, 4.5, 6.0, and 7.5 using 72% sulfuric acid. Each pH-adjusted model solution (1 ml) was brought into contact with $[P_{666,14}][DBP]$, and VFA extraction was quantified. Wastewater fermentation under methanogenic mode as described previously was used to produce broth with no accumulation of VFAs.[1] The broth was spiked with VFAs to

achieve a similar acid concentration as the model solution and used to determine the extraction of VFAs in ILs.

2.4. Computational study of VFA–IL interaction

Structural optimization of acetic acid, propionic acid, butyric acid, hexanoic acid, and ILs including [$P_{666,14}$][DBP] and [$P_{666,14}$]Cl was carried out *via* density functional theory (DFT) using the TmoleX software package (version 23.1.0). To generate the necessary files for COSMO-RS calculations, a single-point DFT analysis was executed utilizing the Becke Perdew 86 (BP86) along with the Triple-Zeta Valence with Polarization (TZVP) parameters. These Cosmo files were then transferred to COSMOthermX (version 23.0.0). All subsequent COSMO-RS analyses utilized the BP_TZVP_23.ctd parameterization file for calculations. The generated COSMO files were then used as input to calculate the sigma profiles, sigma potentials of the isolated molecules, and excess enthalpy (H^E) and logarithmic activity coefficients ln(γ) of VFA solubility in [P666,14][DBP], and [$P_{666,14}$]Cl.[23] In COSMO-RS calculations, the molar fraction of VFAs was set as 0.2 and the molar fraction of ionic liquids was set to 0.8 to mimic the experimental conditions.

The logarithmic activity coefficient ln(γ) of component i is related to the chemical potential as given in the following eqn (1).[24]

$$\ln(\gamma_i) = \left(\frac{\mu_i - \mu_i^0}{RT}\right) \quad (1)$$

where μ_i^0 is the chemical potential of the pure component i, R and T are the ideal gas constant and absolute temperature. The excess enthalpy (H^E) of a binary mixture was calculated using eqn (2).[24,25]

$$H_M^E = \sum x_i H_i^E = \sum x_i [H_{(i,mixture)} - H_{(i,pure)}] \quad (2)$$

where H_M^E is the excess enthalpy of the mixture, defined as the enthalpy difference between component i in the mixture and in the pure state, and the total excess enthalpy of a mixture is the algebraic sum of electrostatic (misfit), hydrogen bonding, and van der Waals interactions.

QTAIM[26] analysis at the bond critical point (BCP) was used to calculate the strength (electron density, $\rho(r)$), and nature of chemical interactions (Laplacian energy density, $\nabla^2\rho(r)$) between the short and longer chain VFAs and the two ionic liquid systems using Multiwfn.[26] Furthermore, to examine the nature of intermolecular interactions in the complex systems, reduced density gradient non-covalent interactions (RDG-NCI) were analyzed using Multiwfn and VMD packages.[27]

2.5. Optimization of enzymatic esterification

A Box–Behnken response surface design of experiment was used to optimize the esterification reactions of VFAs with ethanol in [$P_{666,14}$][DBP] using Novozym 435 as the catalyst. A VFA–IL mixture comprising 50% w/w of VFAs in IL (with equal parts of acetic, propionic, butyric, and hexanoic acids) was prepared and used for the esterification reaction. The esterification process was optimized by evaluating the effect of independent variables including temperature (X_1: 30, 45, and 60 °C), reaction time (X_2: 2, 4, and 6 h), molar ratio of ethanol : acids (X_3: 1 : 1, 3 : 1, and 5 : 1) and enzyme dose (X_4: 2.5, 5, and 7.5 wt%). The total amount of ethanol required at each molar ratio was calculated for each VFA. The amount of enzyme (Novozym 435) required was calculated based on the total reactant weight. For the esterification reaction, the required amounts of reactants in [$P_{666,14}$][DBP] were incubated in a shaker (MAXQ 8000, Thermo Scientific, MA, USA) at a specific temperature. Once the temperature was achieved, the reaction was initiated by adding the enzymes. At the end of the reaction, the mixture was centrifuged to separate the enzymes. An aliquot of the reaction mixture was diluted and used to quantify the residual VFAs. The difference in VFA concentration was used to determine the % conversion of acids into esters.

2.6. Analytical and statistical analysis

The HPLC analysis was conducted using a Dionex Ultimate 3000 equipped with a refractive index detector (RID) (Thermo Fisher, MA, USA). The VFAs were eluted on the Aminex HPX-87H column (Biorad, CA, USA), held at 60 °C, using 4 mM sulfuric acid at 0.6 ml min^{-1}, and detected using an RID (55 °C). The VFAs were identified and quantified by comparison with pure VFA standards. The Box–Behnken response surface design of experiment and statistical data analysis was performed using the Minitab Statistical Software, Version 16 (Pennsylvania State University, USA).

3 Results and discussion

3.1. IL selection and VFA extraction

Six hydrophobic ILs based on the reported cations and anions used for VFA extraction were used for initial screening. The ILs were first evaluated for their immiscibility in water. It was observed that [$P_{666,14}$][DMP], [$P_{444,6}$]Cl, [$P_{444,1}$][TMP] and [$C_{12}C_1$IM][DCA] were miscible in water, whereas [$P_{666,14}$][DBP] and [$P_{666,14}$]Cl were immiscible in water and formed two phases upon standing. Hence [$P_{666,14}$][DBP] and [$P_{666,14}$]Cl were selected as IL candidates to determine their VFA extraction capacity.

[$P_{666,14}$][DBP] and [$P_{666,14}$]Cl were mixed with a model VFA solution (1 : 10 w/v) to quantify the VFA extraction capacity of each IL. As shown in Fig. 1, both [$P_{666,14}$][DBP] and [$P_{666,14}$]Cl have similar extraction capacities for hexanoic acid (68.7 mg per g IL and 68.2 mg per g IL, respectively). However, [$P_{666,14}$][DBP] extracts more shorter chain VFAs:acetic acid (21.4 mg g^{-1} *vs.* 15.5 mg per g IL), propionic acid (44.2 mg per g IL *vs.* 36.3 mg per g IL) and butyric acid (62.7 mg per g IL *vs.* 57.3 mg per g IL) compared to [$P_{666,14}$]Cl. As [$P_{666,14}$][DBP] has relatively higher VFA extraction capacity than [$P_{666,14}$]Cl, [$P_{666,14}$][DBP] was selected as the extraction solvent for further studies. Upon repeated extraction of VFAs by contacting the VFA loaded [$P_{666,14}$][DBP] with the fresh model solution, a total VFA extraction of 842.77 mg per g IL has been achieved, which is significantly higher than the literature (Table 1).

As observed in Fig. 1a, VFA extraction was dependent on the carbon chain length of organic acids. The hydrophobicity of the

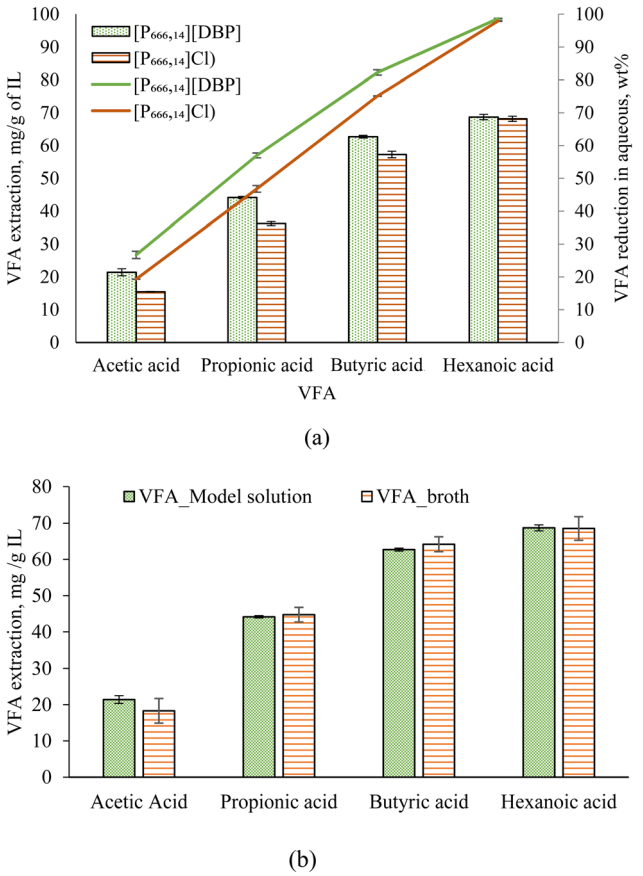

Fig. 1 VFA extraction from aqueous solution in ILs (a) comparison of VFA extraction in $[P_{666,14}][DBP]$ and $[P_{666,14}]Cl$ (bar graph represents primary *Y* axis, and line graph represents secondary *Y* axis) and (b) comparison of VFA extraction in $[P_{666,14}][DBP]$ from the model solution and broth.

VFA increases with increased carbon chain length, which favors the interaction with the hydrophobic ILs. For $[P_{666,14}][DBP]$, a near complete extraction of available hexanoic acid was observed, followed by extraction of about 62% butyric acid, 44% propionic acid, and 21% acetic acid from the model solution. To determine the impact of fermentation broth on VFA extraction, VFA spiked broth with complex cations and anions including calcium, magnesium, potassium, phosphorus, sulfate, and

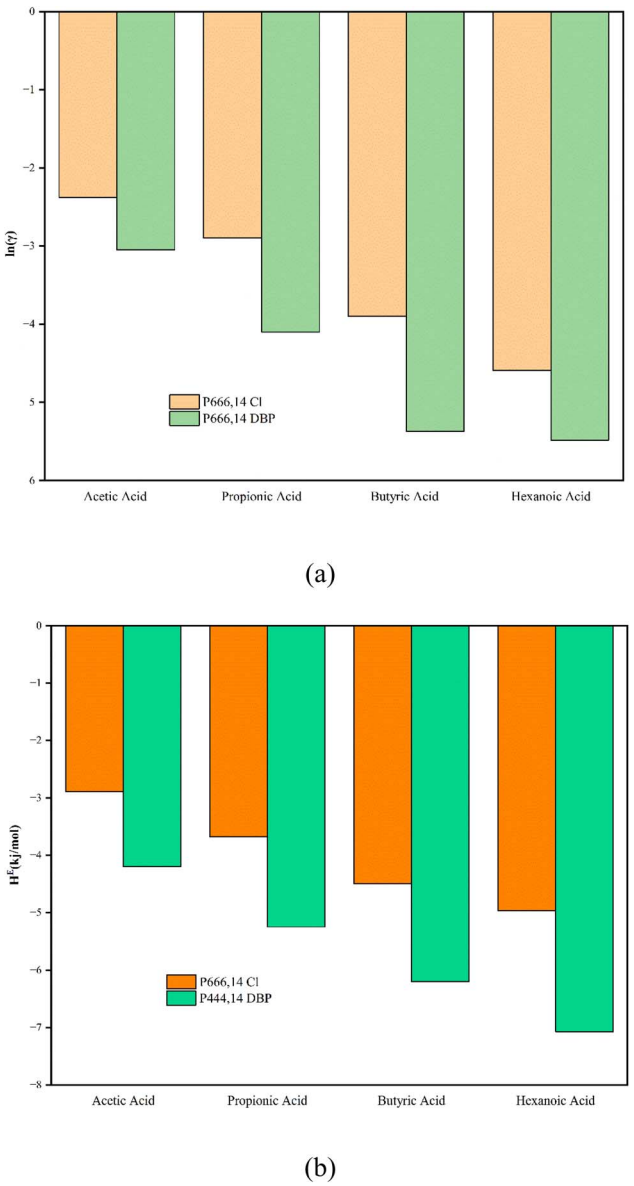

Fig. 2 Calculated thermodynamic properties of VFA and IL interactions: (a) the activity coefficients ln(γ) of the binary mixtures between VFA and selected ILs predicted by COSMO-RS at $T = 298.15$ K, and (b) energetic contributions to the excess enthalpy (H^E) kcal mol^{-1} of the binary mixtures between VFA and selected ILs predicted by COSMO-RS at $T = 298.15$ K.

Table 1 Comparison of VFA extraction efficiency using different ILs

IL cation	IL anion	VFA	IL : VFA volume ratio	VFA extraction	Reference
$[P_{666,14}]$	Dibutyl phosphate	0.8% v/v (acetic acid, propionic acid, butyric acid, and hexanoic acid, each)	1 : 10	842.8 mg per g IL	This work
$[P_{666,14}]$	Bis-2,4,4-(trimethylpentyl) phosphinate	0.25% v/v (lactic acid, acetic acid, propionic acid, and butyric acid)	3 : 5	100 mg per g IL	13
$[P_{666,14}]$	Dicyanamide	19.8 g per L acetic acid	1 : 10	48.4 mg per g IL	15
$[P_{666,14}]$	Chloride	10 g per L (acetic acid and butyric acid)	2 : 1 (20% IL in dodecane)	190–250 mg per g IL (acetic acid), 330–460 mg per g IL (butyric acid)	16

nitrate[1] was used as the substrate for extraction with [$P_{666,14}$][DBP]. As shown in Fig. 1b, VFA extraction from the broth was comparable to that observed for the model solution. It has been reported that the coextraction of other anions from simulated fermentation broth in Cyphos IL104 ([$P_{666,14}$][Phos]) significantly reduced the VFA extraction capacity.[13] In this study, the coextraction of other components of the broth was not quantified since they did not interfere with the VFA extraction to the IL.

The thermodynamic properties such as excess enthalpy (H^E) and logarithmic activity coefficients ln(γ) were calculated using the COSMO-RS method and used to predict VFA solubility in ILs. The H^E is a useful thermodynamic property for measuring the difference in the strength of interactions between dissimilar molecules such as VFAs and ILs while ln(γ) values are often used as a quantitative descriptor for the dissolution power of a solvent. In the literature, ln(γ) has been reported as the dominating parameter in determining the solubilization capability of a solvent and has also been successfully employed in previous studies to predict the solubility of complex solutes such as cellulose and lignin in ILs.[28,29] Therefore, both H^E and ln(γ) parameters were calculated for the long and short-chain VFAs in ILs. Fig. 2a and b report the activity coefficients and excess enthalpy between chloride and DBP based anions with the VFAs respectively. The calculated H^E and ln(γ) values for [$P_{666,14}$][DBP] were significantly smaller (*i.e.*, more negative) than those for [$P_{666,14}$]Cl, indicating that [$P_{666,14}$][DBP] had a stronger affinity for VFAs. The anion showed a greater influence on the dissolution capability of VFAs in the ILs. For ILs with the same cation and different anions, such as [$P_{666,14}$][DBP] and [$P_{666,14}$]Cl the values of excess enthalpies and activity coefficients increased (negative magnitude) as the alkyl carbon chain of fatty acid length increased. The extraction of VFAs

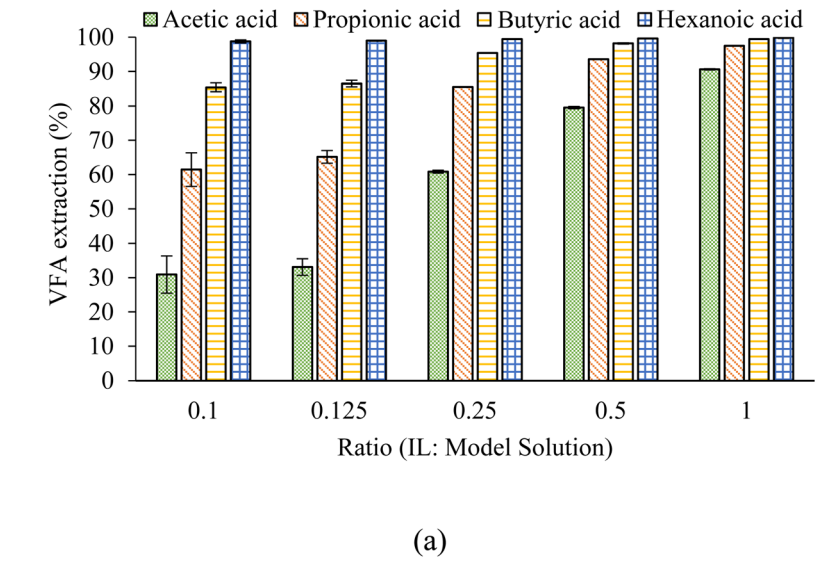

Fig. 3 VFA extraction in [$P_{666,14}$][DBP] at different volume ratios of IL : model solution at fixed initial VFA concentration (0.8% v/v) (a) VFA extraction as % (b) VFA extraction as mg VFA per g IL.

followed the following order of extraction: hexanoic acid > butyric acid > propionic acid > acetic acid, which is consistent with the experimental values.

The results of single-step VFA extraction at different ratios of IL : model solution are presented in Fig. 3. At a fixed initial VFA concentration (0.8% v/v), a higher ratio of IL : model solution resulted in a higher VFA extraction. At a ratio of 0.25 and above, >60% acetic acid, >80% propionic acid, and >90% butyric acid and hexanoic acid were extracted. Higher IL amount gives over 90% extraction of VFAs but due to excess of IL compared to VFA, the VFA extraction in mg VFA per g IL is low. The highest VFA extraction (196.9 mg VFA per g IL) was achieved with a ratio of 0.1 (IL : model solution) followed by 188.4 mg per g IL at a ratio of 0.125. Thus, a ratio of 0.1 provides an economical approach to achieve high VFA extraction at low solvent usage.

As shown in Fig. 4, the VFA extraction in $[P_{666,14}][DBP]$ was found to be dependent on the initial pH of the model solution. The highest VFA extraction was achieved at pH 3.0, however, the extraction achieved at pH values of 1.5 and 4.5 were not statistically significant from pH 3.0 ($p > 0.05$). Above pH 4.5, 55–57% of hexanoic acid was extracted, whereas extraction of acetic acid, propionic acid, and butyric acid was less than 12%. Multiple mechanisms including ion exchange and hydrogen bonding have been proposed for the extraction of organic acids using ILs. At pH below the pK_a of VFAs, the molecular form of weak acids will be the predominant species, thereby suggesting hydrogen bonding as the interaction mechanism between IL and VFAs. Our results corroborate the mechanism reported for Cyphos IL104 ($[P_{666,14}][Phos]$).[13] The authors also proposed an ion-exchange mechanism of acetic acid extraction for IL containing Cl (Cyphos IL101, $[P_{666,14}]Cl$) and Br (Cyphos IL102, $[P_{666,14}]Br$) as the anion. However, ion exchange results in the leaching of IL anion into an aqueous solution, which will have a negative impact on IL reuse. A similar trend was observed for organic solvents such as *n*-octane and dodecane, wherein the VFA extraction was much less at pH 6 compared to pH 3.[16]

3.2. Quantum theory of atoms in molecule and non-covalent interaction analysis

The concept of RDG analysis is articulated using eqn (3), which focuses on the study of electron density in regions characterized by both low electron density (ρ) and minimal gradient values.[30,31]

$$\mathrm{RDG} = \frac{1}{2(3\pi^2)^{1/3}} \frac{|\nabla\rho|}{\rho^{4/3}} \quad (3)$$

This equation sets the basis for NCI analysis, which interprets spikes in RDG as indicators of various weak interactions. Utilizing RDG for NCI analysis can explain and quantify multiple weak interactions, such as H-bonds, vdW, and dispersion interactions. The RDG scatter graph plotted against the electron density modified by the sign of the second eigenvalue of the electron density $[\mathrm{sign}(\lambda_2)\rho]$ unveils a spectrum of weak interactions. These interactions are depicted through RDG isosurfaces and scatter plots, which display changes from positive to negative $[\mathrm{sign}(\lambda_2)\rho]$ values for different compounds, as shown in Fig. 5a–d using M06-2X/def2-TZVP level of theory with D3BJ dispersion correction. Different colored peaks indicate different types of interactions [blue: ($\lambda_2 < 0$), green: ($\lambda_2 \cong 0$), and red: ($\lambda_2 > 0$)]. Blue areas are linked with strong, attractive forces like hydrogen/halogen bonds and electrostatic interactions, while red areas signify strong steric repulsion from nonbonded overlap. The intermediary, or transition, areas track van der Waals interactions, such as dispersion forces and dipole–dipole interactions that are dominant in longer chain VFA interaction with ionic liquids.

The RDG analysis revealed that a mix of hydrogen bonds and van der Waals (vdW) interactions exists between ionic liquids and VFAs, showing several distinct regions on the scatter plot. The blue color in the range of −0.02 and −0.05 atomic units (a.u.) represents the strong noncovalent interaction between the fatty acids and IL. The significant dense blue color spikes occur due to a stable H-bond or ionic interaction between the hydrogen atom of the carboxyl group attached to acetic and hexanoic acids with chloride anion, as shown in Fig. 5a and b. However, vdW or

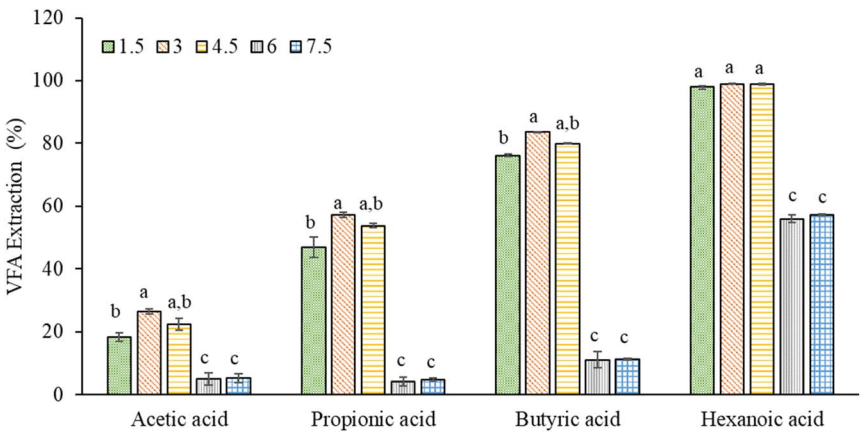

Fig. 4 Effect of the initial pH of VFA model solution on extraction using $[P_{666,14}][DBP]$. Alphabets on top of bars represent statistical significance ($p < 0.05$), where a represents the highest VFA extraction (%) value followed by b, and c. Values sharing an alphabet are not significantly different from each other.

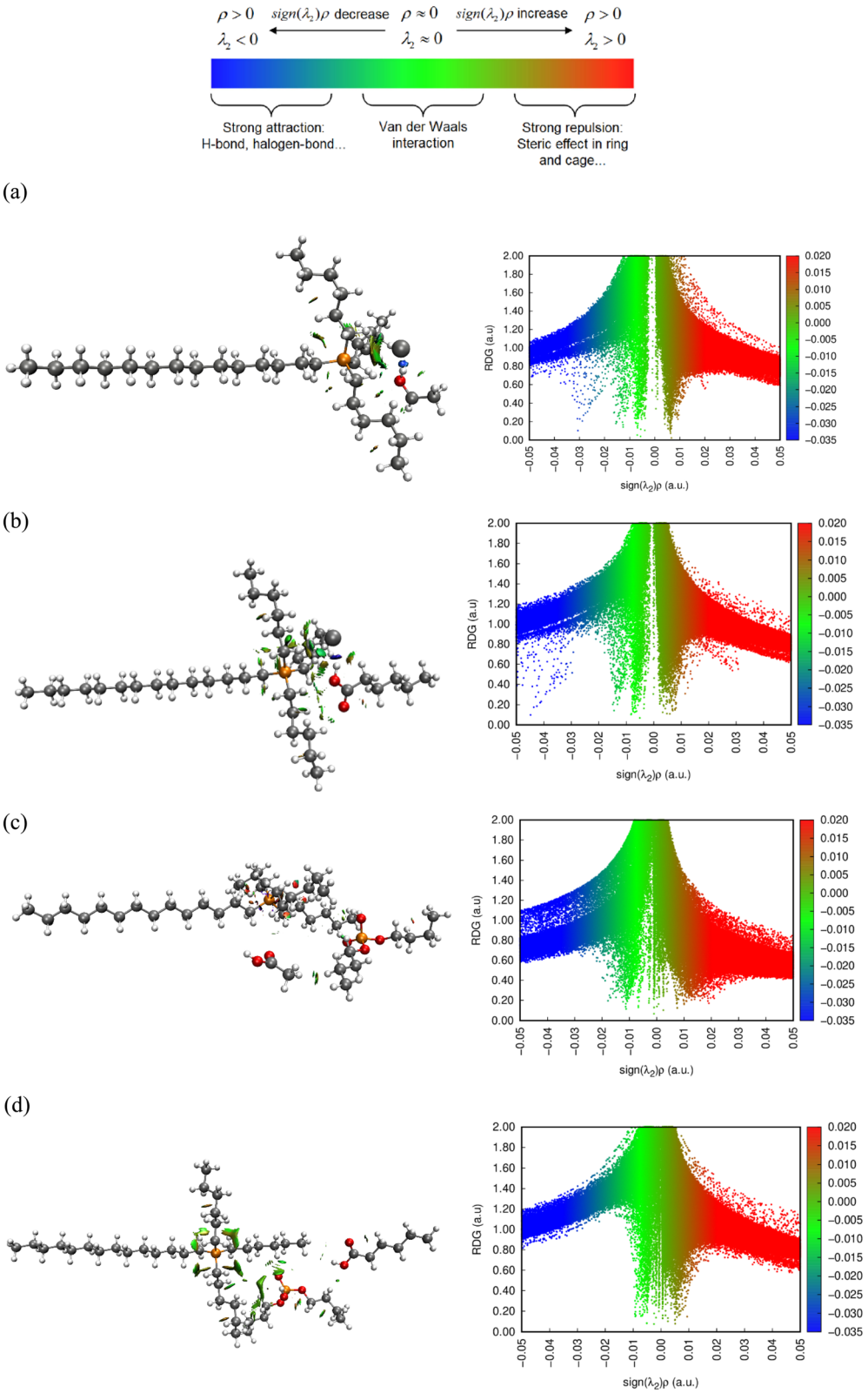

Fig. 5 RDG isosurfaces and scatter graphs of the structures of (a) $[P_{666,14}]Cl$ and acetic acid, (b) $[P_{666,14}]Cl$ and hexanoic acid, (c) $[P_{666,14}][DBP]$ and acetic acid, (d) $[P_{666,14}][DBP]$ and hexanoic acid, at the M06-2X/def2-TZVP level of theory with D3BJ dispersion correction.

dispersion interactions dominated the interaction of acetic acid or hexanoic acid with $[P_{666,14}][DBP]$, as depicted by intermediary dense green color spikes in Fig. 5c and d. The vdW interactions and dispersion-type interaction are the major reasons for the higher solubility of hexanoic acid in ILs. The green markers in a specific range (0 to −0.02 a.u.) hint at vdW and dispersion forces

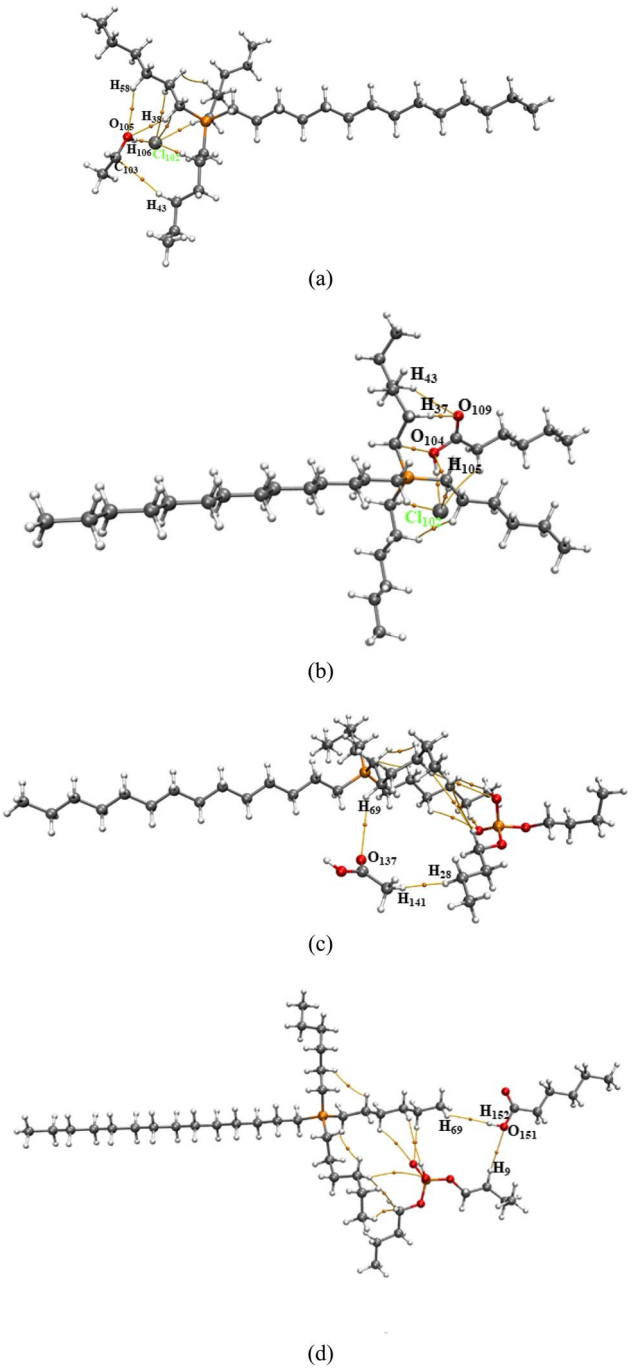

Fig. 6 The complex clusters reveal bond critical points (BCPs) and their corresponding paths of (a) ([$P_{666,14}$]Cl) and acetic acid, (b) ([$P_{666,14}$]Cl) and hexanoic acid, (c) [$P_{666,14}$][DBP] and acetic acid, (d) [$P_{666,14}$][DBP] and hexanoic acid at the M06-2X/def2-TZVP level of theory with D3BJ dispersion correction.

at play, suggesting that the molecules interact weakly without forming strong bonds. Red markers, with values above 0.005 a.u., indicate areas where there are steric hindrances between molecules. This analysis highlights how longer chain fatty acid interactions help in the extraction of VFAs from the aqueous phase using hydrophobic ionic liquids as solvents. The spike present in the range ($\lambda_2 \cong 0.01$) can be attributed to the carbon chain of hexanoic acid and the long alkyl chains of the cation and anion of IL. The dominant presence of the dispersion interactions within the molecular system supports non-covalent interactions devoid of any significant electrostatic interaction between [$P_{666,14}$][DBP] and hexanoic acid.

QTAIM analysis was conducted to decipher hydrogen bonding, vdW, and dispersion type interactions existing in ionic liquids and VFA systems. The magnitude of the electron density at the BCP (3, −1) based on R. F. W. Bader's QTAIM method[32] allowed us to interpret the numerous weak non-covalent interactions between molecules. The BCP seems to be the sites where the electron density gives maxima in two directions and minima in a third direction perpendicular to the former. The electron density (ρ_{BCP}) value indicates the strength of the interaction, and the sign of its Laplacian of electron density ($\nabla\rho_{BCP}^2$) reveals the characteristics of the interaction. A high electron density (ρ_{BCP}) suggests a strong bonding affinity, while a low value indicates weak bonds and a significant distance between atoms. A negative value of the Laplacian of electron density predicts covalent bonding, while a positive value predicts closed-shell interactions such as van der Waals (vdW) interaction, hydrogen bonding, or steric repulsion.[33,34]

QTAIM analysis was employed to understand the mechanisms that drive the extraction of VFAs by ILs. Fig. 6 shows the BCP points between the chloride and DBP anion-based ILs with acetic and hexanoic acids. As reported in Table 2 and depicted in Fig. 6a and b, the electron density, Laplacian of the electron density, and distance between atoms for BCP1 corresponding to the ([$P_{666,14}$]Cl) Cl_{102}–acetic acid H_{106} interaction were 0.0307 a.u., 0.0937 a.u. and 2.1 Å, respectively, which indicates an H-bond interaction between the hydrogen atom of the carboxyl group of VFAs and chloride anion. Similarly, the electron density, Laplacian of the electron density, and distance between atoms for the BCP1 indicate the presence of a hydrogen bond between the ([$P_{666,14}$]Cl) Cl_{102} atom and the hexanoic acid H_{105} atom *via* hydrogen bonding. The rest of the interactions correspond to vdW and dispersion type interactions. In the case of [$P_{666,14}$][DBP] and hexanoic acid, the BCP2 of the H_9–O_{151} interaction has significantly higher electron density at the BCP than the acetic acid systems.

The dominant presence of vdW interactions within the molecular system supports the fact that cation and anion components interact with the hexanoic acid *via* non-covalent interactions devoid of any significant electrostatic interaction. The significant sign(λ_2)ρ values between 0.000 and −0.015 (Fig. 5c and d, green spikes) result from the longer carbon chain being denser in hexanoic acid compared to acetic acid. The chloride anion-based IL and VFA system shows strong hydrogen bonds between the chloride atom and VFA, but interactions get weaker with an increase in the alkyl chain length. In contrast, dispersion-type interactions play the dominant role in the extraction of longer-chain VFA in DBP-based ionic liquids. QTAIM analysis indicates that the DBP anion forms multiple strong interactions with VFAs and can extract high amounts of longer carbon chain VFAs from the fermentation broth, but chloride anion shows strong interaction due to hydrogen

Table 2 Electron density (ρ_{BCP}) and the Laplacian of electron density ($\nabla\rho_{BCP}^2$) at the relevant BCPs in the structures of the studied ionic liquids and fatty acids

Structure	BCP interaction	Type of interaction	Distance (Å)	ρ_{BCP} (a.u.)	$\nabla\rho_{BCP}^2$ (a.u.)
$[P_{666,14}]Cl$ and acetic acid	BCP1: Cl_{102}–H_{106}	H-bonds	2.100	0.0307	0.0937
	BCP2: O_{105}–H_{58}	H-bonds	2.677	0.0050	0.0291
	BCP3: O_{105}–H_{38}	H-bonds	2.240	0.0147	0.0714
	BCP4: C_{103}–H_{43}	Dispersion	2.703	0.0043	0.0134
$[P_{666,14}]Cl$ and hexanoic acid	BCP1: Cl_{102}–H_{105}	H-bonds	1.960	0.0448	0.0697
	BCP2: O_{104}–H_{33}	H-bonds	2.270	0.0145	0.0488
	BCP3: O_{109}–H_{43}	H-bonds	2.620	0.0071	0.0248
	BCP4: O_{109}–H_{37}	H-bonds	2.610	0.0072	0.0211
($[P_{666,14}][DBP]$) and acetic acid	BCP1: O_{137}–H_{69}	vdW	3.720	0.0006	0.0026
	BCP2: H_{141}–H_{28}	Dispersion	2.970	0.0056	0.0173
($[P_{666,14}][DBP]$) and hexanoic acid	BCP1:H_{99}–H_{152}	vdw	2.736	0.0019	0.0064
	BCP2: H_9–O_{151}	H-bonds	2.966	0.0031	0.0109

bonding between chloride anion and –OH of the carboxylic group of VFAs.

3.3. Esterification optimization

Esterification of hexanoic acid was conducted using 0.8% w/w hexanoic acid in $[P_{666,14}][DBP]$ with 5 wt% enzyme loading and resulted in 85.2% conversion of hexanoic acid into esters in 4 h at 60 °C. Increasing the enzyme dose to 10 wt% resulted in a similar conversion (83.4%) yield. The esterification process was optimized using a Box–Behnken response surface design of experiments to maximize the conversion of acids to esters, while minimizing the enzyme dose and temperature using a mixture of VFAs. The experimental design considered three levels for each factor including temperature (X_1: 30, 45, and 60 °C), reaction time (X_2: 2, 4, and 6 h), ethanol : VFA molar ratio (X_3: 1 : 1, 3 : 1, and 5 : 1), and enzyme dose (X_4: 2.5, 5, and 7.5 wt%). The results of the esterification reactions are presented in Table 3. The esterification reaction is dependent on the interaction of acids and ethanol with the active site of enzymes. As observed from the data (Table 3), a higher ester conversion was achieved for hexanoic acid followed by butyric acid, propionic acid, and acetic acid. For acid-catalyzed esterification of slaughterhouse

Table 3 Optimization of VFA esterification in $[P_{666,14}][DBP]$ using Box–Behnken design of experiments

	Experimental conditions				Conversion of acid to ester (%)			
Run no.	Temperature (°C) (X_1)	Time (h) (X_2)	Molar ratio (X_3)	Enzyme dose (wt%) (X_4)	Acetic acid	Propionic acid	Butyric acid	Hexanoic acid
1	30	4	3	7.5	$35.6 \pm 1.3^{a,b}$	$45.1 \pm 1.1^{a,b}$	48.4 ± 3.6^{a}	78.6 ± 0.5^{a}
2		4	3	2.5	24.9 ± 1.3^{c}	36.8 ± 1.1^{c}	$30.9 \pm 2.4^{b,c}$	72.8 ± 0.2^{c}
3		4	5	5	$36.4 \pm 2.2^{a,b}$	47.2 ± 1.7^{a}	27.9 ± 2.6^{c}	$76.6 \pm 0.1^{a,b}$
4		4	1	5	40.2 ± 2.0^{a}	$44.6 \pm 1.3^{a,b}$	39.0 ± 1.5^{b}	$76.3 \pm 0.4^{a,b}$
5		2	3	5	$29.4 \pm 3.2^{b,c}$	$40.1 \pm 0.8^{b,c}$	37.2 ± 1.6^{b}	71.2 ± 0.8^{c}
6		6	3	5	$31.6 \pm 2.5^{a,b}$	$43.0 \pm 1.8^{a,b}$	$39.6 \pm 0.1^{a,b}$	75.9 ± 0.9^{b}
7	45	6	1	5	$41.4 \pm 2.8^{a,b}$	54.3 ± 4.6^{a}	62.9 ± 4.1^{a}	83.6 ± 2.7^{a}
8		6	3	2.5	$32.9 \pm 4.5^{a,b}$	47.3 ± 1.1^{a}	66.1 ± 1.8^{a}	80.0 ± 6.7^{a}
9		4	5	7.5	$43.0 \pm 1.2^{a,b}$	55.5 ± 1.6^{a}	59.0 ± 1.3^{a}	85.0 ± 5.1^{a}
10		2	5	5	$39.7 \pm 9.1^{a,b}$	53.6 ± 4.2^{a}	65.4 ± 0.1^{a}	84.3 ± 0.2^{a}
11		4	5	2.5	32.4 ± 0.3^{b}	46.4 ± 0.1^{a}	58.8 ± 3.1^{a}	85.2 ± 0.5^{a}
12		6	3	7.5	$42.2 \pm 9.8^{a,b}$	61.0 ± 2.2^{a}	77.0 ± 6.5^{a}	83.5 ± 4.9^{a}
13		4	3	5	$37.6 \pm 1.0^{a,b}$	52.6 ± 1.3^{a}	72.6 ± 3.6^{a}	83.3 ± 0.6^{a}
14		4	1	7.5	$45.3 \pm 6.3^{a,b}$	52.6 ± 7.6^{a}	62.6 ± 7.4^{a}	84.2 ± 6.2^{a}
15		6	5	5	39.7 ± 0.6^{a}	47.6 ± 4.8^{a}	70.2 ± 6.0^{a}	85.7 ± 1.0^{a}
16		4	1	2.5	$51.3 \pm 0.2^{a,b}$	56.7 ± 1.0^{a}	65.8 ± 3.6^{a}	85.4 ± 5.6^{a}
17		2	1	5	$43.9 \pm 3.0^{a,b}$	51.6 ± 5.9^{a}	58.7 ± 8.9^{a}	82.4 ± 7.8^{a}
18		2	3	7.5	$34.3 \pm 1.2^{a,b}$	48.8 ± 0.4^{a}	62.8 ± 2.3^{a}	77.1 ± 1.5^{a}
19		2	3	2.5	$33.6 \pm 0.5^{a,b}$	47.8 ± 2.8^{a}	63.3 ± 3.8^{a}	77.4 ± 0.1^{a}
20	60	2	3	5	$27.1 \pm 5.0^{b,c}$	$40.8 \pm 4.7^{a,b}$	$58.3 \pm 4.4^{a,b}$	74.2 ± 0.3^{b}
21		6	3	5	$38.7 \pm 0.2^{a,b}$	$47.3 \pm 1.4^{a,b}$	$67.7 \pm 3.0^{a,b}$	$81.4 \pm 1.3^{a,b}$
22		4	3	7.5	$37.2 \pm 1.9^{a,b}$	49.9 ± 4.0^{a}	71.1 ± 2.2^{a}	82.8 ± 0.7^{a}
23		4	3	2.5	25.6 ± 1.9^{c}	38.1 ± 0.8^{b}	56.8 ± 0.5^{b}	$77.1 \pm 0.8^{a,b}$
24		4	1	5	44.8 ± 0.8^{a}	$48.0 \pm 2.6^{a,b}$	56.3 ± 0.5^{b}	$80.5 \pm 3.9^{a,b}$
25		4	5	5	$38.9 \pm 5.5^{a,b}$	$46.4 \pm 5.4^{a,b}$	$66.1 \pm 5.6^{a,b}$	$79.4 \pm 1.3^{a,b}$

The superscripts on numbers: a–c represent statistical significance ($p < 0.05$) where a represents the highest VFA conversion (%) value followed by b and c.

blood VFA with methanol, a yield of ~35% methyl acetate, ~40–52% methyl propionate, methyl iso-butyrate and methyl butyrate, and ~50% of methyl iso-valerate was reported in the literature using 80% VFA concentration and 1 : 0.3 : 0.5 ratio of VFA : sulfuric acid : methanol.[35] Using Brønsted acidic IL (1-methyl-2-pyrrolidonium hydrogen sulfate, [Hnmp][HSO_4]), 28–67% conversion of acetic acid into esters was reported under different experimental conditions compared to 90% achieved by using sulfuric acid as the catalyst (without IL).[22] Under the optimized conditions (50 °C, 1 : 3 VFA to alcohol, 2% w/w enzyme, and 2 h reaction time), 90% conversion of hexanoic acid to ethyl hexanoate was reported in a solvent-free system.[36] In another study, 86% esterification was achieved for acid-catalyzed esterification of acetic acid in [$P_{666,14}$][Tf_2N].[15] These results suggest that the esterification efficiency is dependent on VFA carbon chain length and the presence of a single *vs.* mixture of VFA in the reaction system.

Optimal conditions for higher conversion were identified at each temperature by ANOVA and Tukey's post-hoc analysis. At 30 °C, 7.5 wt% enzyme, and ethanol : VFA molar ratio of 3 : 1 a higher ester yield (35.6–78.6%) was obtained in 4 h (run 1).

At 45 °C, higher conversions were observed by using 5 wt% enzyme with a molar ratio of 5 : 1 in 6 h (run 15), however, it was not significantly different when the molar ratio was decreased to 3 : 1 and using 4 h of reaction time at the same enzyme dose (run 13). For 60 °C, higher conversion of hexanoic, butyric, and propionic acids was noted by using 7.5 wt% enzyme and a 3 : 1 molar ratio in 4 h (run 22). However, by increasing the molar ratio to 5 and reducing the enzyme dose to 5 wt% (run 25), a similar conversion has been achieved. The full quadratic regression coefficients for ethyl acetate, ethyl propionate, ethyl butyrate, and ethyl hexanoate are provided in eqn (4)–(7), respectively.

$$\begin{aligned}\text{Ethyl acetate (\%)} = {} & 36.29 + 1.21X_1 + 2.08X_2 - 3.06X_3 \\ & + 3.63X_4 - 3.66{X_1}^2 - 1.46{X_2}^2 + 7.13{X_3}^2 \\ & - 0.93{X_4}^2 + 2.35X_1X_2 - 0.55X_1X_3 \\ & + 0.32X_1X_4 + 0.60X_2X_3 \\ & + 0.55\ X_2X_4 + 4.15X_3X_4 \end{aligned} \quad (4)$$

$$\begin{aligned}\text{Ethyl propionate (\%)} = {} & 50.99 + 1.15X_1 + 1.86X_2 \\ & - 0.92X_3 + 3.68X_4 - 7.33{X_1}^2 \\ & - 0.92{X_2}^2 + 2.28{X_3}^2 - 0.53{X_4}^2 \\ & + 0.91X_1X_2 - 1.07X_1X_3 + 0.88X_1X_4 \\ & - 2.12X_2X_3 + 2.09X_2X_4 + 3.30X_3X_4 \end{aligned} \quad (5)$$

$$\begin{aligned}\text{Ethyl butyrate (\%)} = {} & 67.87 + 12.77X_1 + 3.57X_2 \\ & + 0.18X_3 + 3.71X_4 - 15.96{X_1}^2 \\ & - 0.37{X_2}^2 + 4.32{X_3}^2 - 1.20{X_4}^2 \\ & + 1.74X_1X_2 + 5.23X_1X_3 - 0.81X_1X_4 \\ & + 0.15X_2X_3 + 1.57X_2X_4 + 0.87X_3X_4 \end{aligned} \quad (6)$$

$$\begin{aligned}\text{Ethyl hexanoate (\%)} = {} & 81.29 + 1.99X_1 + 2.16X_2 \\ & + 0.31X_3 + 1.31X_4 - 4.73{X_1}^2 \\ & - 1.28{X_2}^2 + 3.01{X_3}^2 - 0.26{X_4}^2 \\ & + 0.58X_1X_2 - 0.34X_1X_3 - 0.04X_1X_4 \\ & + 0.05X_2X_3 + 0.33X_2X_4 + 0.26X_3X_4 \end{aligned} \quad (7)$$

Among the assessed variables, temperature, reaction time, and enzyme dosage were identified as significant factors influencing the conversion of butyric and hexanoic acids into esters ($p < 0.05$). Regarding acetic and propionic acids, only enzyme dosage ($p < 0.05$) exhibited a significant impact on the conversion, in contrast to temperature ($p = 0.1$) and reaction time ($p = 0.01$). Upon conducting ANOVA and Tukey's post-hoc analysis of the optimal conditions at 30 °C (run 1), 45 °C (runs 13 and 15), and 60 °C (run 22), it was observed that conversions at 45 and 60 °C were not significantly different from the lowest values observed at 30 °C ($p < 0.05$). As the upstream fermentation temperature was set at 30 °C, the enzymatic conversions were carried out at this temperature using a higher molar ratio (5 : 1) and enzyme dosage (7.5 wt%) suggested by the model. Under these conditions, significant conversions of 38.3%, 47.1%, 63.2%, and 83.7% for acetic acid, propionic acid, butyric acid, and hexanoic acid, respectively, into esters were achieved. These conversion rates are comparable to those obtained at 45 and 60 °C. Thus, the optimized approach offers alternative experimental conditions aiming at minimizing the energy requirements of the extraction and esterification process.

4 Conclusion

Among the evaluated ILs, [$P_{666,14}$][DBP] and [$P_{666,14}$]Cl were selected as the extraction solvents due to their immiscibility in water. [$P_{666,14}$][DBP] exhibited a superior VFA extraction capacity compared to [$P_{666,14}$]Cl, achieving an overall VFA extraction capacity of approximately 0.8 g per g IL. The thermodynamic parameters for VFA extraction calculated using the COSMO-RS model were observed to agree with experimental values. The VFA extraction in IL depends on the carbon chain length of VFAs and the pH of the medium, while the presence of other fermentation broth components did not interfere with VFA extraction. Thereafter, NCI-RDG and QTAIM analysis indicates that DBP anions form dominating van der Waals (vdW) and dispersion interaction with VFAs and can extract a higher amount of longer chain VFA from the fermentation broth. However, the chloride anion-based IL extracts VFAs due to hydrogen bonding between the chloride anion and the carboxylic group of VFAs. The longer chain VFA is also more soluble in DBP-based ILs compared to chloride anion-based IL as vdW interactions dominate earlier systems. This analysis highlighted the critical role of hydrogen bonding, vdW, and dispersion-type interactions in the extraction of VFAs using ILs. Furthermore, the enzymatic esterification of VFAs in ILs was optimized using a Box–Behnken design. Under the optimized conditions (30 °C, 6 h, ethanol : VFA molar ratio = 5 : 1, enzyme dosage: 7.5 wt%), conversion rates of 38.3%, 47.1%, 63.2%, and 83.7% were achieved for acetic acid, propionic acid, butyric acid, and hexanoic acid, respectively. This work identifies a promising process that utilizes hydrophobic ILs for VFA extraction from dilute fermentation broth and *in situ* esterification. Currently, achieving high extraction and conversion of all VFAs in a single IL system is limited by the preference for longer alkyl chain acids. However, this limitation also presents an opportunity to separate or enrich VFAs with longer chain

length (C4–C6). A combination of different separation approaches is expected to recover all the VFAs. Efforts are also underway for chain elongation of the shorter chain VFAs to maximize the concentration of a medium chain VFAs (C4, C6 or higher). In such a case, the process developed here will be readily applicable. Future work including the recovery and reuse of ILs, as well as enzyme recycling is crucial for advancing the process towards industrial applications.

Data availability

All the data supporting this article are included in this manuscript.

Author contributions

RS: conceptualization, investigation, methodology, formal analysis, data curation, writing – original draft, writing – review & editing; NK: investigation, methodology, formal analysis, data curation, writing – original draft, BS: supervision, writing – review & editing; PP: funding acquisition, writing – review & editing; KS: supervision, writing – review & editing; NS: conceptualization, funding acquisition, supervision, writing – review & editing.

Conflicts of interest

BAS is a co-founder and has a financial interest in Illium Technologies, Caribou Biofuels, and Erg Bio.

Acknowledgements

The authors would like to thank Novozyme North America Inc. (part of Novonesis) for providing the enzyme for this study. This work was supported by the Industrial Efficiency & Decarbonization Office (IEDO) within the US DOE's Office of Energy Efficiency and Renewable Energy (DE-EE0009504). ABPDU would also like to thank the support from The Bioenergy Technologies Office (BETO) within the US DOE's Office of Energy Efficiency and Renewable Energy. This work was also supported by the Joint BioEnergy Institute, U.S. Department of Energy, Office of Science, Biological and Environmental Research Program under Award Number DE-AC02-05CH11231 with Lawrence Berkeley National Laboratory. Sandia National Laboratories is a multi-mission laboratory managed and operated by National Technology and Engineering Solutions of Sandia, LLC, a wholly owned subsidiary of Honeywell International, Inc., for the U.S. Department of Energy's National Nuclear Security Administration under contract DE-NA0003525. The views and opinions of the authors expressed herein do not necessarily state or reflect those of the United States Government or any agency thereof. Neither the United States Government nor any agency thereof, nor any of their employees, makes any warranty, expressed or implied, or assumes any legal liability or responsibility for the accuracy, completeness, or usefulness of any information, apparatus, product, or process disclosed or represents that its use would not infringe privately owned rights.

References

1 A. Damodara Kannan and P. Parameswaran, *J. Water Proc. Eng.*, 2021, **43**, 102234.
2 S. Agnihotri, D.-M. Yin, A. Mahboubi, T. Sapmaz, S. Varjani, W. Qiao, D. Y. Koseoglu-Imer and M. J. Taherzadeh, *Bioengineered*, 2022, **13**, 1249–1275.
3 V. K. Varghese, B. J. Poddar, M. P. Shah, H. J. Purohit and A. A. Khardenavis, *Sci. Total Environ.*, 2022, **815**, 152500.
4 A. Patel, A. Mahboubi, I. S. Horváth, M. J. Taherzadeh, U. Rova, P. Christakopoulos and L. Matsakas, *Front. Microbiol.*, 2021, **12**, 614612.
5 J.-d.-r. Choi, H. N. Chang and J.-I. Han, *Biotechnol. Lett.*, 2011, **33**, 705–714.
6 C. Mengmeng, C. Hong, Z. Qingliang, S. N. Shirley and R. Jie, *Bioresour. Technol.*, 2009, **100**, 1399–1405.
7 C. M. Spirito, H. Richter, K. Rabaey, A. J. M. Stams and L. T. Angenent, *Curr. Opin. Biotechnol.*, 2014, **27**, 115–122.
8 M. Atasoy, I. Owusu-Agyeman, E. Plaza and Z. Cetecioglu, *Bioresour. Technol.*, 2018, **268**, 773–786.
9 W. S. Lee, A. S. M. Chua, H. K. Yeoh and G. C. Ngoh, *Chem. Eng. J.*, 2014, **235**, 83–99.
10 M. Blahušiak, Š. Schlosser and J. Marták, *Sep. Purif. Technol.*, 2013, **119**, 102–111.
11 Á. Bóna, P. Bakonyi, I. Galambos, K. Bélafi-Bakó and N. Nemestóthy, *Membranes*, 2020, **10**, 252.
12 J. Marták and Š. Schlosser, *Sep. Purif. Technol.*, 2007, **57**, 483–494.
13 E. Reyhanitash, B. Zaalberg, S. R. A. Kersten and B. Schuur, *Sep. Purif. Technol.*, 2016, **161**, 61–68.
14 E. Alkaya, S. Kaptan, L. Ozkan, S. Uludag-Demirer and G. N. Demirer, *Chemosphere*, 2009, **77**, 1137–1142.
15 S. J. Andersen, J. K. Berton, P. Naert, S. Gildemyn, K. Rabaey and C. V. Stevens, *ChemSusChem*, 2016, **9**, 2059–2063.
16 T. Xing, S. Yu, J. Tang, H. Liu, F. Zhen, Y. Sun and X. Kong, *Energies*, 2023, **16**, 785.
17 A. P. Sarnaik, S. Shinde, A. Mhatre, A. Jansen, A. K. Jha, H. McKeown, R. Davis and A. M. Varman, *Sci. Rep.*, 2023, **13**, 10766.
18 Z. Khan, F. Javed, Z. Shamair, A. Hafeez, T. Fazal, A. Aslam, W. B. Zimmerman and F. Rehman, *J. Ind. Eng. Chem.*, 2021, **103**, 80–101.
19 Q. Wang, N. H. Al Makishah, Q. Li, Y. Li, W. Liu, X. Sun, Z. Wen and S. Yang, *Front. Bioeng. Biotechnol.*, 2021, **9**, 661694.
20 Š. Schlosser, J. Marták and M. Blahušiak, *Chem. Pap.*, 2018, **72**, 567–584.
21 A. C. Blaga, A. Tucaliuc and L. Kloetzer, *Membranes*, 2022, **12**(8), 771.
22 B. Zhou, Y. Fang, H. Gu, S. Zhang, B. Huang and K. Zhang, *Front. Chem. Eng. China*, 2009, **3**, 211–214.
23 F. Eckert and A. Klamt, *AIChE J.*, 2002, **48**, 369–385.
24 K. A. Kurnia, S. P. Pinho and J. A. P. Coutinho, *Ind. Eng. Chem. Res.*, 2014, **53**, 12466–12475.

25 M. Gonzalez-Miquel, M. Massel, A. DeSilva, J. Palomar, F. Rodriguez and J. F. Brennecke, *J. Phys. Chem. B*, 2014, **118**, 11512–11522.
26 T. Lu and F. Chen, *J. Comput. Chem.*, 2012, **33**, 580–592.
27 W. Humphrey, A. Dalke and K. Schulten, *J. Mol. Graphics*, 1996, **14**, 33–38.
28 E. C. Achinivu, M. Mohan, H. Choudhary, L. Das, K. Huang, H. D. Magurudeniya, V. R. Pidatala, A. George, B. A. Simmons and J. M. Gladden, *Green Chem.*, 2021, **23**, 7269–7289.
29 A. Casas, J. Palomar, M. V. Alonso, M. Oliet, S. Omar and F. Rodriguez, *Ind. Crops Prod.*, 2012, **37**, 155–163.
30 E. R. Johnson, S. Keinan, P. Mori-Sánchez, J. Contreras-García, A. J. Cohen and W. Yang, *J. Am. Chem. Soc.*, 2010, **132**, 6498–6506.
31 B. A. Marekha, O. N. Kalugin and A. Idrissi, *Phys. Chem. Chem. Phys.*, 2015, **17**, 16846–16857.
32 R. F. W. Bader, *Chem. Rev.*, 1991, **91**, 893–928.
33 B. Bankiewicz, P. Matczak and M. Palusiak, *J. Phys. Chem. A*, 2012, **116**, 452–459.
34 W. Kohn, A. D. Becke and R. G. Parr, *J. Phys. Chem.*, 1996, **100**, 12974–12980.
35 J. Plácido and Y. Zhang, *Waste Biomass Valorization*, 2018, **9**, 1767–1777.
36 S. D. Gawas, N. Lokanath and V. K. Rathod, *Biocatalysis*, 2018, **4**, 14–26.